EMP Theoretical Notes

TN 369

23 May 2022

NUMERICAL SIMULATION OF THE HEMP ENVIRONMENT[1]

Aleksandr I. Golubev, Anton V. Terekhin, Vladimir A. Terekhin, Egor V. Uvarov

Russian Federal Nuclear Center - All-Russia Research Institute of Experimental Physics, Sarov, 607200 Russia, Email: terekhin.vladimir.1947@gmail.com;

William A. Radasky,

Metatech Corporation, 358 S. Fairview Ave. Suite E, Goleta, CA 93117, USA, Email: wradasky@aol.com

ABSTRACT

A model based on a self-consistent solution of the Boltzmann kinetic equation for electrons together with Maxwell's equations has been developed to determine the characteristics of the high-frequency component of an electromagnetic pulse (EMP) generated in air by a pulse of gamma radiation from a high-altitude nuclear explosion. This approach makes it possible to correctly take into account the initial spectral-angular distribution of the generated electrons and positrons, as well as their further interaction with the medium and the generated electric field. Examples are given that illustrate the importance of taking into account nonlinear, nonstationary, and kinetic effects in predicting the EMP parameters of a high-altitude nuclear explosion.

INTRODUCTION

In the mid 1960's a classical work by W. J. Karzas and R. Latter [1] was published. It described, for the first time, the mechanism of generating an electromagnetic pulse (EMP) of a high-altitude nuclear explosion ($H > 30$ km) based on the cophased emission (in the Earth's magnetic field) of relativistic electrons generated due to Compton scattering of gamma-quanta and absorbed at a height of 15 to 30 km. As for identifying EMP parameters of a high-altitude nuclear explosion to solve a multi-dimensional system of Maxwell's equations, a high-frequency approximation based on a short duration of a gamma radiation burst $c\tau_\gamma \sim 100$ m, as compared to the spatial scale $\Delta \sim 10$ km of a varying atmospheric density, was proposed. The aforementioned approach allowed estimating the amplitude-time characteristics of a high-altitude EMP (HEMP), which are the basis, to the present day, for specifying requirements on the resistance to nuclear explosion EMP effects.

In the mid 1990's a physical model was proposed in [2] and further developed in [3]-[6] to describe the propagation of a high-power EMP to the atmosphere and ionosphere. The model was based on a self-consistent solution of the Boltzmann kinetic equation for electrons in combination

[1] The paper is based on materials of the report "*Development of Modern Technologies for the Calculation of HEMP Parameters Accounting for Non-linear, Non-stationary and Kinetic Effects*" (January 2004) executed under the subcontract S0303-1021-03 between Sarov Labs and Metatech, Inc.

with Maxwell's equations. The Boltzmann equation was numerically solved for the following two groups of electrons:

- Slow electrons (< 1-10 keV), which were described by a classical two-polynomial expansion assuming that the electron distribution function anisotropy is weak;
- Fast electrons (> 1-10 keV), which were described with a modified method for macroparticles with consideration of the electromagnetic field effect on their motion, energy losses in the continuous slowing-down approximation, and multiple scattering.

Using this model, the self-consistent electrodynamic EMP propagation problem was implemented based on the selection of the main and slowly varying pulse parameters in the solution of Maxwell's equations, i.e. the amplitude and phase [3].

This new approach allowed calculating parameters of the avalanche ionization evolution in gas (N_2) preliminarily ionized by an external source of gammas. It was demonstrated [4] that even a relatively small number of fast electrons could decrease the breakdown electric field amplitude by an order of magnitude. A considerable drop in the electric stability of air due to gamma and X-ray radiation is caused by the relativistic electron avalanche development. Theoretical studies of this phenomenon were described in [7]. In particular, the requirement of a large space ($\geq$ 100 m) for such avalanche development was shown and because of this fact the effect was not observed under laboratory conditions. At the same time, HEMP parameters may be strongly affected by the avalanche growth of the concentration of relativistic electrons escaping under the effect of electromagnetic fields [2].

The same model was also used to investigate the propagation of sub-nanosecond and high-amplitude EMPs in air [5] – [6]. It was shown that because of its short duration, such a pulse has a higher breakdown threshold and, therefore, an EMP with amplitude ~ 1 MV/m could propagate to a height of 100 km without appreciable energy losses.

The research of the mid 1970's (e.g. [8]) demonstrates that in the near zone of atmospheric NE the generated polarized electric field has a limited amplitude due to the electron avalanche development. This requires accounting for self-consistent effects to predict HEMP parameters.

The emerging spatial and temporal picture of the polarization charge differentiation caused by the self-consistent motion of Compton electrons might be viewed as a giant spherical capacitor having a kilometer radius and a distance of dozens of meters between the "plates". This capacitor expands with the speed of light from the explosion center and under certain conditions might serve as an efficient accelerator of positrons, which emerge due to the generation of pairs (from high-energy gammas in the U^{235} fission spectrum) and are captured by the electric field and accelerated up to ultra-relativistic energies [9].

Obviously, all of the effects above (and many others) might manifest themselves during the HEMP generation both in the source region, i.e. at distances of several kilometers to nuclear explosion, and in the deposition region, or the enhanced ionizion region (H=15-30km), where gamma quanta are mainly absorbed. All of this requires the development of a self-consistent kinetic model to describe processes of the HEMP generation and propagation that would allow accounting for nonstationary, non-linear, and kinetic effects. So, the present paper is focused on the development of such a model to address the early-time (E1) HEMP behavior.

Section 1 presents the HEMP generation problem setup for the self-consistent solution of Maxwell's equation system in the high-frequency approximation [1] and the Boltzmann kinetic equation for electrons. Similarly to solutions described in [2] – [6], the Boltzmann equation is solved for the following two groups of electrons:

- Slow electrons (< 1-10 keV) described using the elliptic representation of the Boltzmann equation [10], which we modified to take into consideration the external magnetic field $\vec{B}_0$; and
- Fast electrons (> 1-10 keV) described in the continuous slowing-down and multiple scattering approximation [11].

Section 2 gives results of

- the verification of a complete set of cross-sections for collisions of electrons with air molecules (which are the input data for the numerical code) using the in-lab experimental data;
- the analysis of the radiation-induced conductivity dynamics of reaching the equilibrium; and
- the investigation of the electron escape effect on the avalanche ionization kinetics in calculations of the radiation-induced conductivity.

To illustrate the importance of the effects above, Section 3 presents the calculated characteristics of EMP generated by a point instantaneous source of gammas.

A gamma ray source with a peak production rate of $\Gamma_m = 10^{31} - 10^{33}$ MeV/s has the spectrum coinciding with the U^{235} fission spectrum and is located at a height of H=15-30 km above the Earth surface. This is a quite representative problem to study physical processes governing the early-time (E1) HEMP behavior.

1. A SELF-CONSISTENT MODEL TO DESCRIBE HEMP

The HEMP generation and propagation problem can be divided into two parts [6]. The first one is the analysis (based on the numerical solution of the Boltzmann kinetic equation) of the dynamics of electrons and positrons in the electric and magnetic field with collisions between these particles and neutral molecules taken into account. The distribution function $f_\alpha(t,\vec{r},\vec{p})$ for particles α $(\alpha = e,p)$ allows finding their current density $\vec{j}_\alpha = e_\alpha \int d\vec{p}\cdot(\vec{v}\cdot f_\alpha)$, where $\vec{v} = \vec{p}/m\gamma$ and $\vec{p}$ are the particle velocity and momentum, respectively, and $\gamma = \sqrt{1 + p^2/m^2c^2}$.

The current density $\vec{j} = \sum j_\alpha$ is required for the second part to describe the space and time evolution of the electric, $\vec{E}$ and magnetic, $\vec{B}$ fields behind the EMP front moving at the speed of light. Using variables $\vec{r}$ and $\tau = t - (\vec{n}\cdot\vec{r})/c$, where $\vec{n}$ is a unit vector directed from the explosion center to the point of interest, the system of Maxwell's equations describing the dynamics of generated electromagnetic fields takes the form:

$$\begin{aligned} \frac{\partial}{\partial\tau}\vec{B} - (\vec{n}\times\frac{\partial\vec{E}}{\partial\tau}) &= -c(\nabla\times\vec{E}) \\ \frac{\partial}{\partial\tau}\vec{E} + (\vec{n}\times\frac{\partial\vec{B}}{\partial\tau}) + 4\pi\vec{J} &= c(\nabla\times\vec{B}). \end{aligned} \tag{1.1}$$

The path lengths of electrons and positrons in atmosphere and lower ionosphere are much less than the typical scale of a varying air density. Hence, the spatial dependence of the particle distribution function can be ignored and the locally uniform kinetic equation can be solved:

$$\left[1 - \frac{(\vec{n}\cdot\vec{v})}{c}\right]\frac{\partial f_\alpha}{\partial\tau} + e_\alpha\cdot\left[\vec{E} + \frac{\vec{v}}{c}\times(\vec{B}+\vec{B}_0)\right]\cdot\frac{\partial f_\alpha}{\partial\vec{p}} = N\cdot J^{st}(f_\alpha) + S_\alpha \tag{1.2}$$

where $\vec{B}_0$ is geomagnetic field, N is the concentration of molecules, J^{st} is the integral of Boltzmann collisions, and S_α is a source of electrons and positrons generated by gamma rays from NE.

The self-consistent solution scheme for the HEMP problem is presented in Fig. 1.1. Obviously, an ability to solve a 3D problem[2] is highly unlikely, even with the use of modern computers and advanced methods for parallel computations. So, to describe the early-time HEMP behavior, we use three reasonable simplifications.

[2] A 3D (in the coordinate space) system of Maxwell's equations for the electromagnetic fields is considerably diverse in scale, and the 3D (in the momentum space) integral/differential Boltzmann equation varies within a wide range of particle energies from eVs (conductivity electrons) up to hundreds of MeVs (escaping electrons and accelerated positrons)

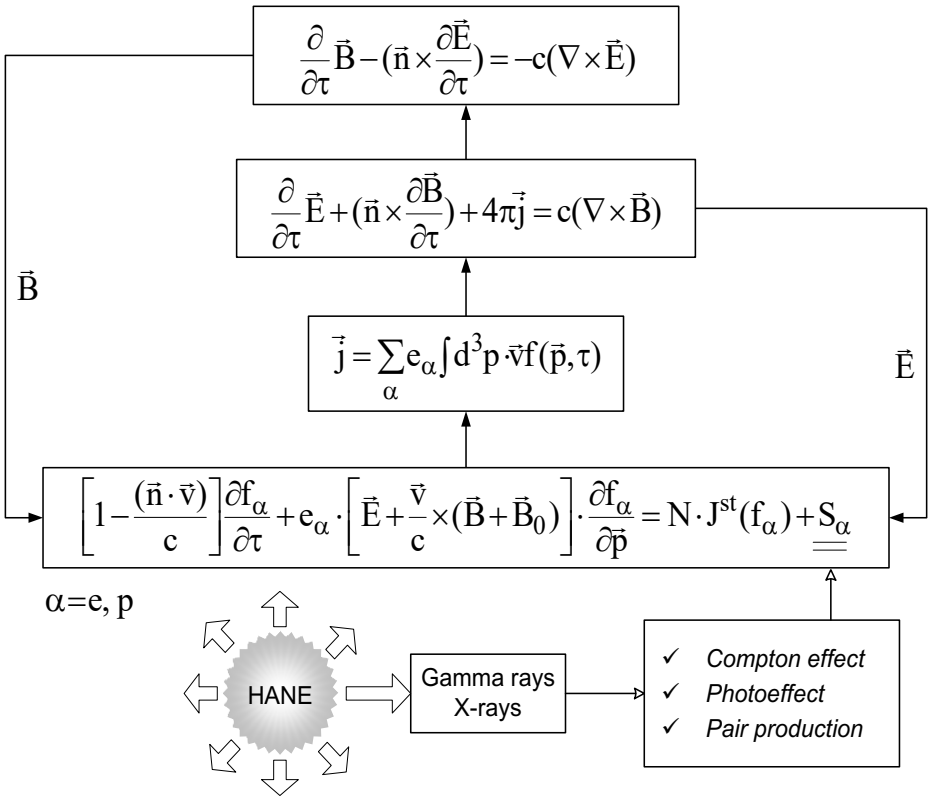

Fig. 1.1. *Basic equations*.

1.1. Boltzmann Equation

Today, we have a lot of developed numerical methods to solve the multi-dimensional Boltzmann kinetic equation for particles in different energy spectra. They have been used rather efficiently to solve various problems in the gas-discharge and ionospheric plasma physics. However, the problem above has some specific feature requiring special methods to solve equation (1.2), namely, electrons generated due to the atmosphere ionization by gamma rays have energies within a wide range of values, from eVs to hundreds of MeVs, with all parts of the energy range being significant and requiring special consideration.

We are not aware of the works proposing methods to find the distribution function for electrons (positrons) in such a wide range of varying energies. For this reason, two developed approximate approaches were offered in [2] – [6] to solve the kinetic equation using a single scheme justified from viewpoint of physics.

All particles fall into one of the two energy groups. Slow particles with the energies $\varepsilon \le 10$ keV are described in a non-relativistic approximation. It is possible to use the so-called elliptical representation of the Boltzmann equation [10], which we generalized for the case of the external magnetic field $\vec{B}_0$. In order to describe kinetics of fast particles (with energies $\varepsilon \ge 10$ keV), the energy loss continuity and angular scattering approximation is used and in case of collisions with molecules (e.g. [11]) the relativistic Fokker-Planck approximation is used for the collision integral

(e. g. [3], [6]). Systems of kinetic equations describing slow and fast particles are correlated through the corresponding boundary conditions with regard to the energy variable, i.e. the transition of particles from one energy group to another and backwards will be possible.

1.1.1. Kinetics of Slow Electrons

Slow electrons are non-relativistic and, therefore, we can omit terms $(\vec{n}\cdot\vec{v})/c$ and $[\vec{v}\times\vec{B}]/c$ in the Lorentz force expression. Indeed, intensities of the electric and magnetic fields are of the same order, while the velocity of slow electrons is much less than the speed of light. So, the kinetic equation for slow electrons takes the form

$$\frac{\partial f}{\partial \tau}-\frac{\partial}{\partial \vec{v}}\left\{\frac{e\vec{E}}{m}+\frac{e}{m}\left[\frac{\vec{v}}{c}\times\vec{B}_0\right]\right\}f=I_{st}(f)+\sum_{\beta}S_{\beta}\,, \tag{1.3}$$

where I_{st} is collision term, and S_{β} denotes sources.

Let us derive equations for the moments of the electron distribution function in its general form. The integration of equation (1.3) with respect to variable $\vec{\Omega}\equiv\vec{v}/v$ gives us the following equation:

$$\frac{\partial n}{\partial \tau}-\frac{e}{m}\vec{E}\int d\vec{\Omega}\vec{\nabla}_v f+\frac{e}{mc}\vec{B}^0\int d\vec{\Omega}\left[\vec{v}\frac{\partial f}{\partial \vec{v}}\right]=I_{st}^0+\sum_{\beta}S_{\beta}^0\,. \tag{1.4}$$

Multiplying equation (1.3) by $\vec{\Omega}$ and then integrating it, we obtain the second equation:

$$\frac{\partial \vec{\Gamma}}{\partial \tau}-\frac{e}{m}\int d\vec{\Omega}\vec{\Omega}\left(\vec{E}\frac{\partial f}{\partial \vec{v}}\right)+\frac{e}{mc}\int d\vec{\Omega}\vec{\Omega}(\vec{B}^0\cdot\left[\vec{v}\frac{\partial f}{\partial \vec{v}}\right])=I_{st}^{(1)}+\sum_{\beta}S_{\beta}^{(1)}\,. \tag{1.5}$$

Here, $n=\int d\vec{\Omega}f,\quad \vec{\Gamma}=\int d\vec{\Omega}\vec{\Omega}f.$

Collision terms I_{st}^0, I_{st}^1 include the elastic scattering process, excitation of air molecules, impact ionization, and attachment of electrons to molecules of O_2. We derive the following expressions for these terms:

$$\begin{aligned}I_{st}^0=N\Bigg\{&\frac{2m}{M}\frac{\partial}{\partial\varepsilon}\left(v\varepsilon Q_{el}n\right)-v(\varepsilon)Q_{at}(\varepsilon)n-\sum_k v(\varepsilon)Q_{ex}^k\cdot n+\\ &\sum_k v(\varepsilon+u_k)Q_{ex}^k(\varepsilon+u_k)n(\varepsilon+u_k)-v(\varepsilon)n(\varepsilon)\sum_k Q_{ion}^k(\varepsilon)+\\ &+\sum_k\int_{2\varepsilon+I_k}^{\varepsilon_c}dT\,v(T)S_k^+(T,\varepsilon)n(T)+\sum_{\ell}\int_{\varepsilon+I_k}^{2\varepsilon+I_k}dT v(T)S_k^+(T,T-\varepsilon-I_k)n(T)\Bigg\},\end{aligned} \tag{1.6}$$

$$\vec{I}_{st}^1=-Nv(\varepsilon)Q_{eff}(\varepsilon)\cdot\vec{\Gamma}.$$

where M is a molecule mass, ε is kinetic energy of electrons, u_k and I_k are thresholds of the molecule excitation and ionization of the k-th level, respectively, $S_k^+(\varepsilon,T)$ is the differential cross-

section of ionization, Q_{el} is the transport cross-section of elastic scattering, $Q^k_{ion}(\varepsilon) = \int_0^{(\varepsilon - I_k)/2} dT S^+_k(\varepsilon, T)$ is the ionization cross-section of a molecule, Q_{at} is the attachment cross-section, and

$$Q_{eff} = Q_{el} + Q_{at} + \sum_k Q^k_{ex} + \sum_k Q^k_{ion}$$

is the effective cross-section. Though these integrals are written for a one-component gas, the generalization to a gas mixture is obvious.

Now, we are ready to use formulas (1.4) and (1.5) to derive the moment equations for elliptical approximations. For convenience, we introduce denotations for some integrals:

$$\vec{\psi}_1 = \int d\vec{\Omega} \frac{\partial f}{\partial \vec{v}}; \ \vec{\psi}_2 = \int d\vec{\Omega} \left[\vec{v} \frac{\partial f}{\partial \vec{v}} \right];$$

$$\vec{\psi}_E = \frac{e}{m} \int d\vec{\Omega}\vec{\Omega} \left(\vec{E} \cdot \frac{\partial f}{\partial \vec{v}} \right); \ \vec{\psi}_B = \frac{e}{mc} \int d\vec{\Omega}\vec{\Omega} \left(\vec{B}^0 \cdot \left[\vec{v} \frac{\partial f}{\partial \vec{v}} \right] \right).$$

In the elliptical approximation we can write

$$f = \frac{b\sqrt{1-\gamma^2}}{1 - \vec{\gamma} \cdot \frac{\vec{v}}{v}}, \tag{1.7}$$

where functions b and $\vec{\gamma}$ depend on v and τ.

For the first two moments, we obtain equations

$$n(v,\tau) \equiv \int d\vec{\Omega} f = \frac{2\pi b\sqrt{1-\gamma^2}}{\gamma} \ln\left(\frac{1+\gamma}{1-\gamma} \right),$$

$$\vec{\Gamma}(v,\tau) = \int d\vec{\Omega}(\vec{\Omega} \cdot f) = \frac{2\pi b\sqrt{1-\gamma^2}}{\gamma} \left[\frac{1}{\gamma} \ln\left(\frac{1+\gamma}{1-\gamma} \right) - 2 \right] \cdot \frac{\vec{\gamma}}{\gamma} \tag{1.8}$$

Introduce variable $X = |\vec{\Gamma}| / n$, for which expression

$$X = \frac{1}{\gamma} - \frac{2}{\ln\left(\frac{1+\gamma}{1-\gamma} \right)}$$

is valid, and obtain

$$\frac{\partial f}{\partial \vec{v}} = \frac{\partial}{\partial v} \vec{\Omega} \frac{b\sqrt{1-\gamma^2}}{\left(1 - \vec{\gamma} \cdot \vec{\Omega}\right)} + \frac{b\sqrt{1-\gamma^2}}{v} \cdot \frac{\vec{\gamma} - \vec{\Omega}\left(\vec{\gamma} \cdot \vec{\Omega}\right)}{\left(1 - \vec{\gamma} \cdot \vec{\Omega}\right)^2}, \ \vec{\psi}_1 = \frac{1}{v^2} \frac{\partial}{\partial v} \left(v^2 \vec{\Gamma} \right), \ \vec{\psi}_2 = 0, \ \vec{\psi}_B = -\frac{e}{mc} \left[\vec{B}^0 \times \vec{\Gamma} \right]$$

$$\vec{\psi}_E = \frac{e}{m} E_j T_{ij} = \frac{e}{m} \cdot \vec{E} \left\{ \frac{\partial}{\partial v} \left[\frac{n}{2} \left(1 - \frac{X}{\gamma} \right) \right] + \frac{n}{2v} \left(1 - \frac{3X}{\gamma} \right) \right\} + \frac{e}{m} \cdot \frac{1}{v^3} \cdot \frac{\partial}{\partial v} \left\{ \frac{v^3 n}{2} \left(\frac{3X}{\gamma} - 1 \right) \frac{(\vec{E} \cdot \vec{\gamma})}{\gamma^2} \vec{\gamma} \right\},$$

where

$$T_{ij} = \left\{ \frac{\partial}{\partial v}\left[\frac{n}{2}\left(1 - \frac{X}{\gamma}\right)\right] + \frac{n}{2v}\left(1 - \frac{3X}{\gamma}\right)\right\}\delta_{ij} + \frac{1}{v^3}\frac{\partial}{\partial v}\left\{ \frac{v^3 n}{2}\left(\frac{3X}{\gamma} - 1\right)\frac{\gamma_i \gamma_j}{\gamma^2}\right\}.$$

Thus, equations for n and $\vec{\Gamma}$ in the elliptical approximation have the form:

$$\begin{cases} \dfrac{\partial n}{\partial \tau} - \dfrac{e}{m}\cdot\dfrac{1}{v^2}\cdot\dfrac{\partial}{\partial v}\left[v^2\left(\vec{E}\cdot\vec{\Gamma}\right)\right] = I_{st}^{(0)} + \sum_{\beta} S_{\beta}^{(0)} \\ \dfrac{\partial \vec{\Gamma}}{\partial \tau} - \dfrac{e}{m}\cdot\dfrac{1}{v^2}\cdot\dfrac{\partial}{\partial v}\left[\dfrac{nv}{2}\left(\dfrac{3X}{\gamma} - 1\right)\cdot\dfrac{(\vec{E}\cdot\vec{\gamma})}{\gamma^2}\cdot\vec{\gamma}\right] - \\ \dfrac{e}{m}\vec{E}\cdot\left\{\dfrac{\partial}{\partial v}\left[\dfrac{n}{2}\left(1 - \dfrac{X}{\gamma}\right)\right] + \dfrac{n}{2v}\left(1 - \dfrac{3X}{\gamma}\right)\right\} - \dfrac{e}{mc}\left[\vec{B}_0 \times \vec{\Gamma}\right] = \vec{I}_{st}^{(1)} + \sum_{\beta}\vec{S}_{\beta}^{(1)} \end{cases} \quad (1.9)$$

Note that with $\vec{B}^0 \to 0$ equations (1.9) transform into those obtained by Richley [10] for n and $\vec{\Gamma}$ in the elliptical approximation.

1.1.2. Kinetics of Fast Electrons

We can write the following kinetic equation for the distribution function of fast electrons, f_f (sources in the right-hand part are omitted, for simplicity):

$$\frac{\partial f_f}{\partial t} + v\vec{\Omega}\frac{\partial f_f}{\partial \vec{r}} - e\frac{\partial}{\partial \varepsilon}\left\{\left[(\vec{\Omega}\cdot\vec{E}) + \frac{F_D}{e}\right]\cdot v f_f\right\} - e\frac{\partial}{\partial \vec{\Omega}}\left\{\vec{\Omega}\times\left[\vec{E}\times\vec{\Omega} + \frac{v}{c}(\vec{B} + \vec{B}_0)\right]\cdot\frac{f_f}{p}\right\}, \quad (1.10)$$
$$= N\cdot J_f^{st} + S_{ion}^f + S_{\gamma}^f$$

where F_D is the dynamic friction force, which governs energy losses in the continuous slowing-down approximation according to the Bethe-Bloch formula.

Sources S_{ion}^f and S_{γ}^f in the right-hand part of equation (1.10) describe the generation of fast electrons in the ionization process of neutral molecules due to their collisions with electrons and under the impact of gamma/X-ray radiation from the NE. Finally, the term J_f^{st} is a part of the collisions integral that describes the angular scattering of fast electrons.

The left-hand part of equation (1.10) describes the trajectory of a particle in the phase space under the influence of the Lorentz force and the dynamic friction force, F_D. This part of the equation is easily simulated with the macro particles moving along real electrons' trajectories. Certain difficulties should be attributed to the term J_f^{st}, which describes electron collisions and, therefore, their stochastic removal from the deterministic trajectory. This process can be simulated using either the Monte-Carlo method, or the method of macro particles with the way of describing the multiple scattering offered by C. Longmire in [12] – [13] and modified in [3].

As compared to Longmire's model, in the modified model the electric field also affects the variation in the average cosine of the scattering angle, μ_q. Besides, μ_q also has an effect on the degree of varying the macro particle momentum.

$$\begin{cases}\left(1-\dfrac{(\vec{n}\cdot\vec{v}_q)}{c}\right)\dfrac{d\varepsilon_q}{dt}=-v_q F(\varepsilon_q)-e\mu_q v_q\vec{\Omega}_q\cdot\vec{E}\\ \left(1-\dfrac{(\vec{n}\cdot\vec{v}_q)}{c}\right)\dfrac{d\vec{\Omega}_q}{dt}=-\dfrac{ev_q}{p_q}\left[\vec{\Omega}_q\times(\vec{B}+\vec{B}_0)\right]-\dfrac{e}{\mu_q p_q}\left\{\vec{E}-(\vec{\Omega}_q\cdot\vec{E})\vec{\Omega}_q\right\}\\ \left(1-\dfrac{(\vec{n}\cdot\vec{v}_q)}{c}\right)\dfrac{d\mu_q}{dt}=-\mu_q v_q\Sigma_{tr}(\varepsilon_q)-\dfrac{1-\mu_q^2}{p_q}e(\vec{\Omega}_q\cdot\vec{E})\end{cases}\qquad(1.11)$$

To complete the presentation of the approximation approach to describing the dynamics of fast electrons, we should give the explicit form of electron sources in the right-hand part of kinetic equations (1.3) and (1.10) governed by ionization collisions of fast electrons with molecules. Assuming that during the molecule ionization the secondary fast electrons emerge mainly in the direction orthogonal to the ionizing particle momentum, we obtain the following expression for S_{ion}^{f} ($\varepsilon > \varepsilon_g$):

$$S_{ion}^{f}=N\delta(\vec{\Omega})\int_{\varepsilon_g}^{\infty}d\varepsilon_p\int d\vec{\Omega}_p\int_0^1 d\mu_p f_f(\varepsilon_p,\vec{\Omega}_p,\mu_p)v_p s^{+}(\varepsilon_p,\varepsilon).\qquad(1.12)$$

The source $S_{ion}^{s}(\varepsilon<\varepsilon_g)$ of slow electrons resulting from the molecule ionization by fast electrons looks like

$$S_{ion}^{s}=\frac{N}{2\pi(2/m)^{3/2}}\int_{\varepsilon_g}^{\infty}d\varepsilon_p\int d\vec{\Omega}_p\int_0^1 d\mu_p\, f_f(\varepsilon_p,\vec{\Omega}_p,\mu_p)\; v_p s^{+}(\varepsilon_p,\varepsilon).\qquad(1.13)$$

I.1.3. Sources of Fast Electrons

As it was mentioned in the introduction to this paper, fast particles are the result of Compton scattering of gamma quanta by bound electrons of air molecules (the Compton effect), photoabsorption of quanta (the photo effect) and the generation of electron-positron pairs. Assuming that the gamma radiation spectrum is preset as a combination of lines with energies ε_γ^k and a relative number of quanta G_k in these lines, the source of Compton electrons, S_c may be represented in the following form:

$$S_c=\frac{\dot{N}_\gamma^{m}f_\gamma(\tau)}{4\pi r^2}\sum_{k=1}^{K}\frac{G_k}{R_c^k(h)}\exp\left\{-\int_0^r\frac{dr'}{R_t^k(h')}\right\}g_c^k(\vec{p}).\qquad(1.14)$$

R_c^k and R_t^k can be calculated using Tables from [14], while in order to describe $g_c^k(\vec{p})$ (i.e. the energy angular distribution) use the Klein-Nishina-Tamm cross-section.

I.2. Maxwell's Equations

Equations (1) together with equations (1.3) and (1.11) form a closed system, which may be used to analyze the high power EMP propagation through the atmosphere. However, because of a

complicated form of these equations for theoretical and numerical analysis we'll use some approximations to solve Maxwell's equations.

I.2.1. High Frequency Approximation [1], [15]

In a spherical system of coordinates $(\tau = t - r/c, r, \theta, \varphi)$ with its center at the source of explosion, equations (1.1) will look like

$$\begin{cases} \frac{1}{c}\frac{\partial E_r}{\partial \tau} = -\frac{4\pi}{c} j_r + \frac{1}{r\sin\theta}\left[\frac{\partial(\sin\theta \cdot B_\varphi)}{\partial\theta} - \frac{\partial B_\theta}{\partial\varphi}\right] \\ \frac{1}{c}\frac{\partial(E_\theta - B_\varphi)}{\partial \tau} = -\frac{4\pi}{c} j_\theta + \frac{1}{r\sin\theta}\frac{\partial B_r}{\partial\varphi} - \frac{1}{r}\frac{\partial(rB_\varphi)}{\partial r} \\ \frac{1}{c}\frac{\partial(E_\varphi + B_\theta)}{\partial \tau} = -\frac{4\pi}{c} j_\varphi - \frac{1}{r}\frac{\partial B_r}{\partial\theta} + \frac{1}{r}\frac{\partial(rB_\theta)}{\partial r} \\ \frac{1}{c}\frac{\partial B_r}{\partial \tau} = \frac{1}{r\sin\theta}\left[\frac{\partial E_\theta}{\partial\varphi} - \frac{\partial(\sin\theta \cdot E_\varphi)}{\partial\theta}\right] \\ \frac{1}{c}\frac{\partial(E_\varphi + B_\theta)}{\partial \tau} = \frac{1}{r}\frac{\partial(rE_\varphi)}{\partial r} - \frac{1}{r\sin\theta}\frac{\partial E_r}{\partial\varphi} \\ \frac{1}{c}\frac{\partial(B_\varphi - E_\theta)}{\partial \tau} = -\frac{1}{r}\frac{\partial(rE_\theta)}{\partial r} + \frac{1}{r}\frac{\partial E_r}{\partial\varphi} \end{cases} \tag{1.15}$$

By integrating the last two equations with respect to τ, we obtain

$$rB_\varphi = rE_\theta + \frac{\partial}{\partial\theta}\int_{-\infty}^{\tau} E_r c d\tau - \frac{\partial}{\partial r}\int_{-\infty}^{\tau} rE_\theta c d\tau \tag{1.16}$$

$$rB_\theta = -rE_\varphi + \frac{\partial}{\partial r}\int_{-\infty}^{\tau} rE_\varphi c d\tau - \frac{1}{\sin\theta}\frac{\partial}{\partial\varphi}\int_{-\infty}^{\tau} E_r c d\tau \tag{1.17}$$

Substituting the expressions obtained into the 2nd and 3d equations of system (1.15), we obtain the following equations:

$$\frac{\partial}{\partial r}(rE_\theta) = -\frac{2\pi}{c} rJ_\theta + \frac{1}{2}\frac{\partial E_r}{\partial\theta} + \frac{1}{2\sin\theta}\frac{\partial B_r}{\partial\varphi} - \frac{1}{2}\frac{\partial^2}{\partial r\partial\theta}\int_{-\infty}^{\tau} E_r c d\tau + \frac{1}{2}\frac{\partial^2}{\partial r^2}\int_{-\infty}^{\tau} rE_\theta d\tau \tag{1.18}$$

$$\frac{\partial}{\partial r}(rE_\varphi) = -\frac{2\pi}{c} rJ_\varphi + \frac{1}{2\sin\theta}\frac{\partial E_r}{\partial\varphi} - \frac{1}{2}\frac{\partial B_r}{\partial\theta} - \frac{1}{2\sin\theta}\frac{\partial^2}{\partial r\partial\varphi}\int_{-\infty}^{\tau} E_r c d\tau + \frac{1}{2}\frac{\partial^2}{\partial r^2}\int_{-\infty}^{\tau} rE_\varphi c d\tau \tag{1.19}$$

Further, we assume that the behavior of electromagnetic fields in space and time in the problems of interest is such that

$$\left|\frac{1}{c}\frac{\partial}{\partial\tau}\right| >> \left|\frac{\partial}{\partial r}\right|$$

and in Maxwell's equations we'll neglect space derivatives, as compared to time derivatives *of the same quantities*.

Within the high-frequency approximation, since we have

$$rE_\alpha = \frac{\partial}{c\partial\tau}\int_{-\infty}^{\tau} rE_\alpha c d\tau >> \frac{\partial}{\partial r}\int_{-\infty}^{\tau} rE_\alpha c d\tau \qquad \frac{\partial}{\partial r}(rE_\alpha) = \frac{\partial^2}{c\partial\tau\partial r}\int_{-\infty}^{\tau} rE_\alpha c d\tau >> \frac{1}{2}\frac{\partial^2}{\partial r^2}\int_{-\infty}^{\tau} rE_\alpha c d\tau,$$

where $\alpha = \theta, \varphi$, equations for transversal components of the electric field are simplified and take the form:

$$\begin{cases} \frac{\partial}{\partial r}(rE_\theta) = -\frac{2\pi}{c}J_\theta + \frac{1}{2}\frac{\partial E}{\partial\theta} + \frac{1}{2\sin\theta}\frac{\partial B_r}{\partial\varphi} \\ \frac{\partial}{\partial r}(rE_\varphi) = -\frac{2\pi}{c}J_\varphi + \frac{1}{2\sin\theta}\frac{\partial E}{\partial\varphi} - \frac{1}{2}\frac{\partial B_r}{\partial r} \end{cases}, \tag{1.20}$$

where $E \equiv E_r - \int_{-\infty}^{\tau}\frac{\partial E_r}{\partial r}c d\tau$; and formulas (1.16) and (1.17) for transversal components of the magnetic field look lile

$$\begin{cases} rB_\varphi = rE_\theta + \frac{\partial}{\partial\theta}\int_{-\infty}^{\tau} E_r c d\tau \\ rB_\theta = -rE_\varphi - \frac{1}{\sin\theta}\frac{\partial}{\partial\varphi}\int_{-\infty}^{\tau} E_r c d\tau \end{cases}. \tag{1.21}$$

Expressions (1.20) – (1.21) in combination with equations

$$\begin{cases} \frac{1}{c}\frac{\partial E_r}{\partial\tau} = -\frac{4\pi}{c}J_r + \frac{1}{r\sin\theta}\left[\frac{\partial}{\partial\theta}(\sin\theta\cdot B_\varphi) - \frac{\partial B_\theta}{\partial\varphi}\right] \\ \frac{1}{c}\frac{\partial B_r}{\partial\tau} = \frac{1}{r\sin\theta}\left[\frac{\partial E_\theta}{\partial\varphi} - \frac{\partial}{\partial\theta}(\sin\theta\cdot E_\varphi)\right] \end{cases} \tag{1.22}$$

for radial components of the generated electro-magnetic field form a full system of electro-dynamic equations in the high frequency approximation, which can be used to look at parameters of the early-time HEMP behavior.

2. ON THE RADIATION-INDUCED CONDUCTIVITY IN AIR

The approach described above was used to study the radiation-induced air conductivity dynamics in order to:

- verify a complete set of cross-sections of electron-air molecule collisions (which are the input data for the numerical technique) using in-lab experimental data;
- analyze the dynamics of the radiation-induced conductivity reaching the equilibrium; and
- investigate the effect of escaping electrons on the avalanche ionization kinetics in radiation-induced conductivity calculations.

2.1. Verification of the Method Using a Lot of Measurement Data for Nitrogen and Oxygen

In order to verify the proposed model accuracy and demonstrate its capabilities, we calculated the drift velocity (W) and the Townsend coefficient (α/N) in nitrogen with a varying intensity of the external electric field (E/N) within the range of values (1-10^3) Td. The comparison of the calculated results and experimental data is shown in Figs.2.1 - 2.2.

There is a good agreement between the calculated drift velocity, W and experimental data [16]-[19] (see Fig.2.1) with an insignificant, but continuously growing deviation for E/N >100 Td (1 Td = 10^{-17} Vcm^2). This is due to the assumed isotropic nature of inelastic scattering cross-sections. The validity of this statement was demonstrated in [20] for E/N = 800 Td, where it was shown that two assumptions - the inelastic scattering cross-section is a) isotropic and b) has the indicatrix coinciding with the elastic scattering - lead to the discrepancy of values, with experimental data in intermediate position.

Though the kinetic model with the binomial decomposition allows accounting for the inelastic scattering anisotropy, we have almost no data on the indicatrix for molecular gases. So, the deviation shown in Fig.2.1 reasonably demonstrates the accuracy of our model. Besides, the comparison (Fig.2.2) between the calculated Townsend ionization coefficient, $\alpha = \nu_{ion} / W$ and experimental data from [16], [21] - [22] proves the model accuracy.

We calculated the values of drift velocity W, Townsend coefficient α/N and attachment coefficient η / N (three-particle– $e + O_2 + M \rightarrow O_2^- + M$ and dissociative– $e + O_2 \rightarrow O^- + O$) in oxygen with a varying intensity of the external electric field E/N within the range of values (10-10^3) Td. The calculated results and experimental data from [23] – [27] are compared in Figs.2.3 - 2.5.

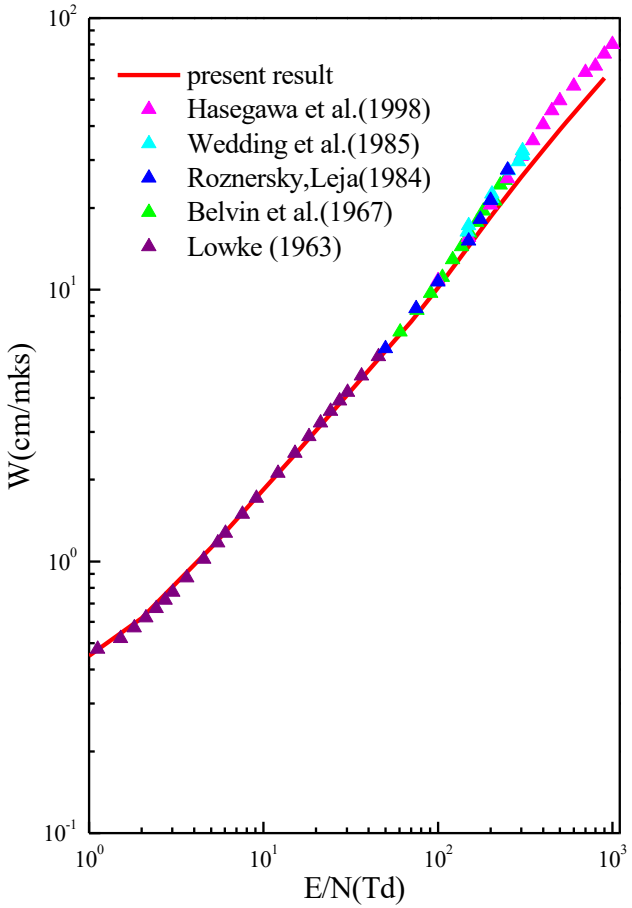

Fig. 2.1. *Dependence of the electron drift velocity, W in molecular nitrogen on the ratio of the applied electric field to the gas density, E/N. Solid line represents simulation results. Triangles are the experimental data.*

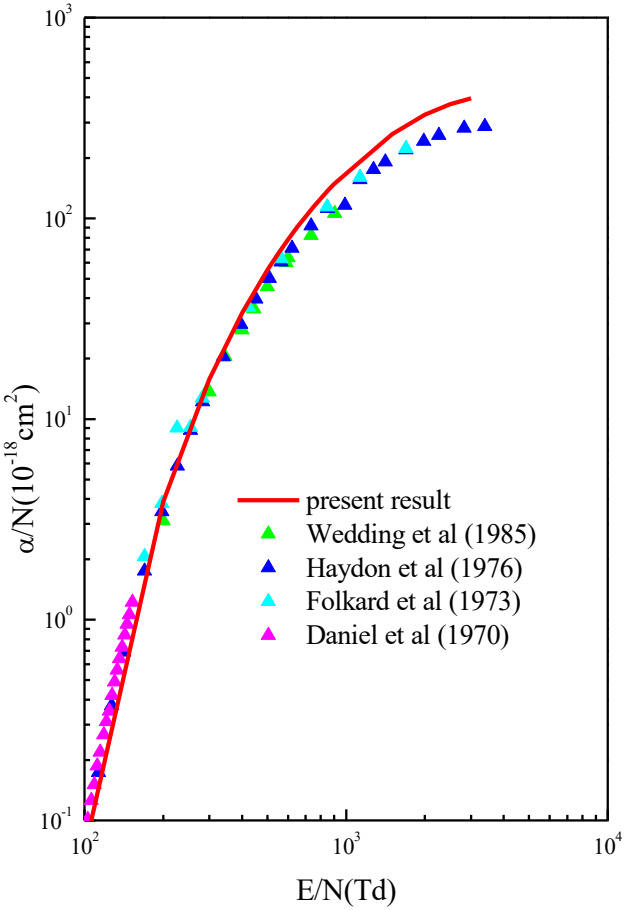

Fig. 2.2. *Dependence of the electron ionization coefficient, a/N in molecular nitrogen on the ratio of the applied electric field to the gas density, E/N. Solid line represents simulation results. Triangles are the experimental data.*

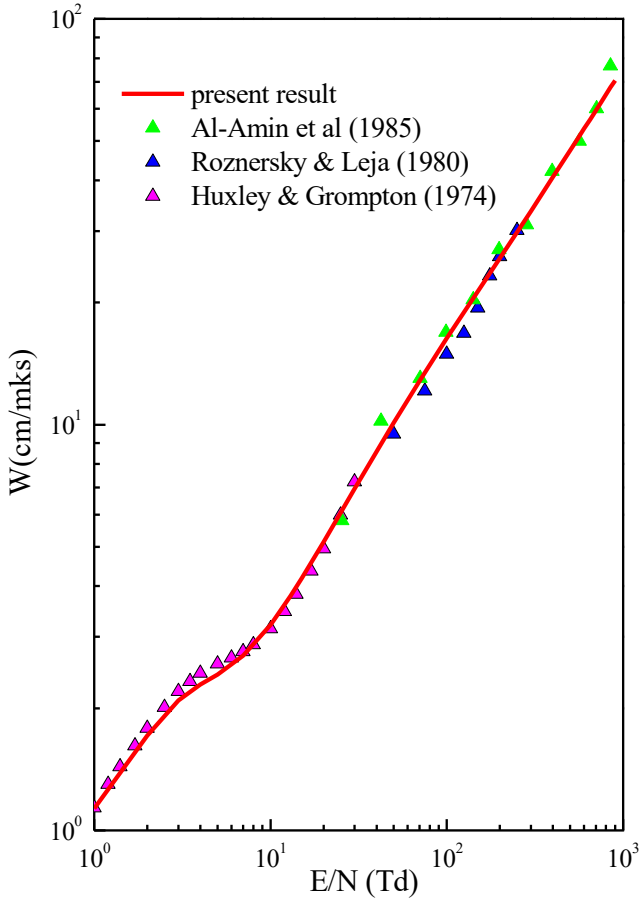

Fig. 2.3. *Dependence of the electron drift velocity, W in molecular oxygen on the ratio of the applied electric field to the gas density, E/N. Solid line represents simulation results. Triangles are the experimental data.*

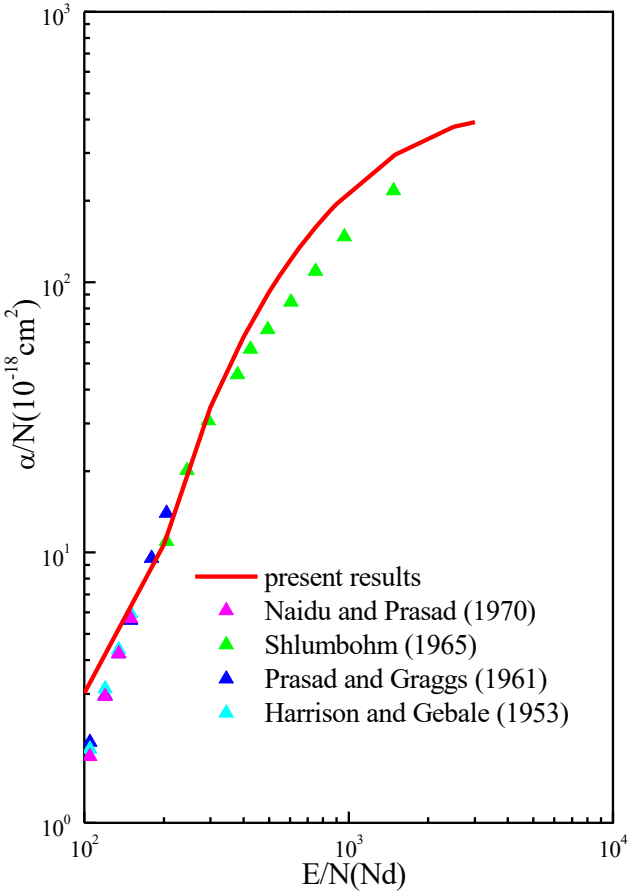

Fig. 2.4. *Dependence of the electron ionization coefficient, a/N in molecular oxygen on the ratio of the applied electric field to the gas density, E/N. Solid line represents simulation results. Triangles are the experimental data.*

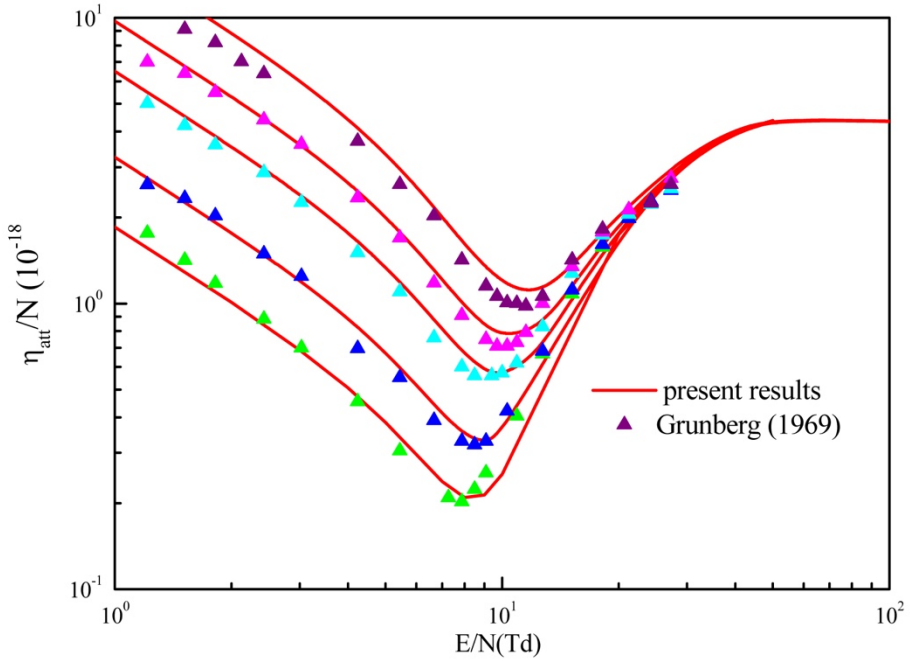

Fig.2.5. *Attachment coefficient* η/N *for electrons in oxygen vs E/N. Solid curves represent simulation results. For comparison, we show the data obtained by Grunberg (1969) and systematized in the review [16].*

Examples in the figures above demonstrate a high accuracy of the model in describing slow electrons. Unfortunately, we have no experimental data on the governing role of fast electrons. There is only one experimental fact - the energy lost by a fast electron (having energy >10 keV) to generate one electron-ion pair does not depend on the electron energy and equals 36 eV for molecular nitrogen and 34 eV for oxygen. This data is in a good agreement with our computation results.

2.2 Numerical Simulation Data on Radiation-Induced Conductivity in Air

For a model point gamma source, we simulated the radiation-induced conductivity dynamics:

- the rate of the gamma-quanta yield varied with time in accordance with formula

$$\Gamma(\tau) = \Gamma_m \cdot \delta(\tau), \tag{2.1}$$

- the energy spectrum of gamma rays was described by formula

$$g(w) = \frac{1}{< E_\gamma >} \times \exp\left(-\frac{w}{< E_\gamma >}\right), \tag{2.2}$$

which approximates the U^{235} fission spectrum, $< E_\gamma > = 1\mathrm{MeV}$,

The calculated dynamic characteristics of electrons governing the radiation-induced conductivity are shown in Figs.2.6–2.7.

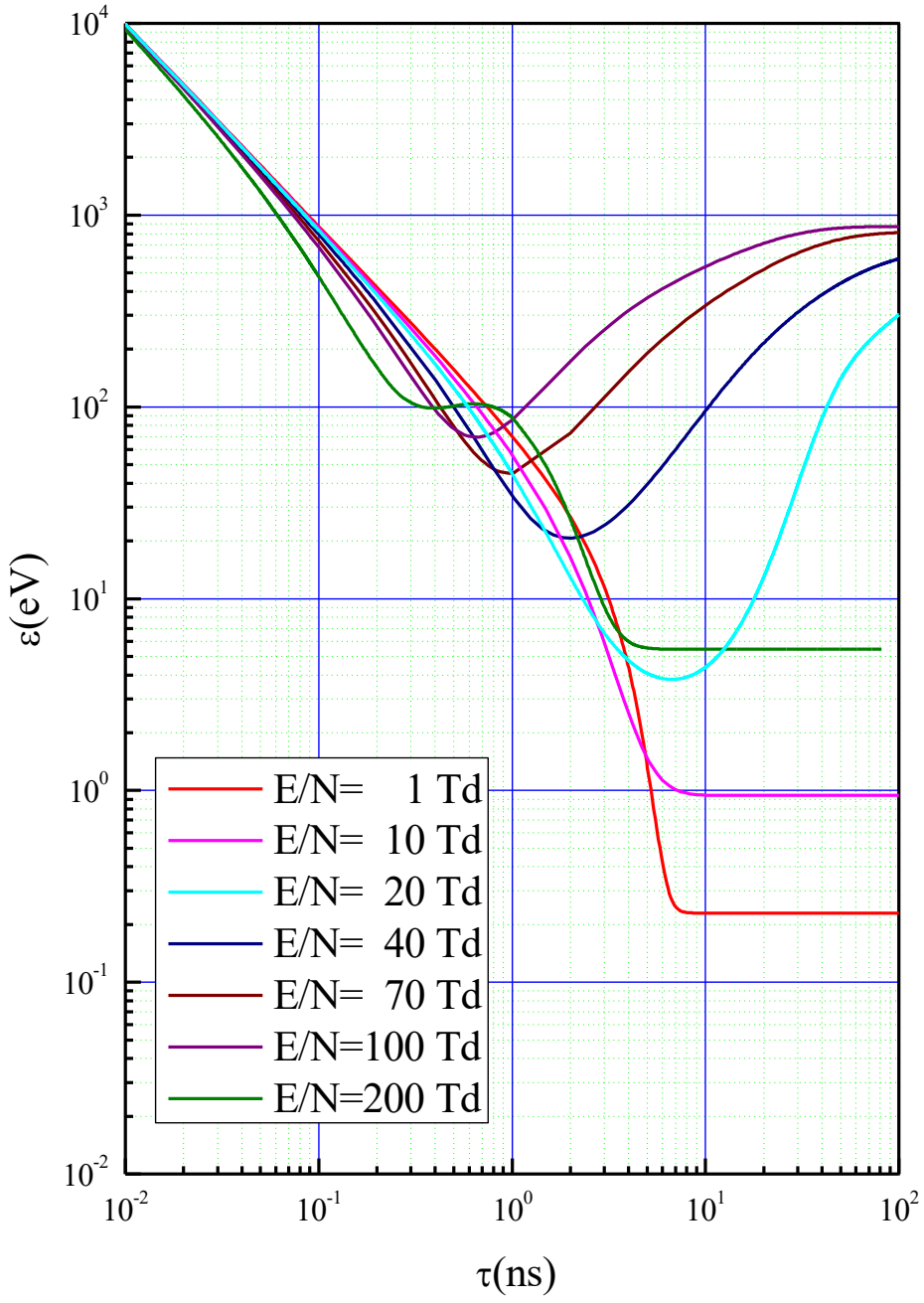

Fig. 2.6. *Electron mean energy <ε> vs time*

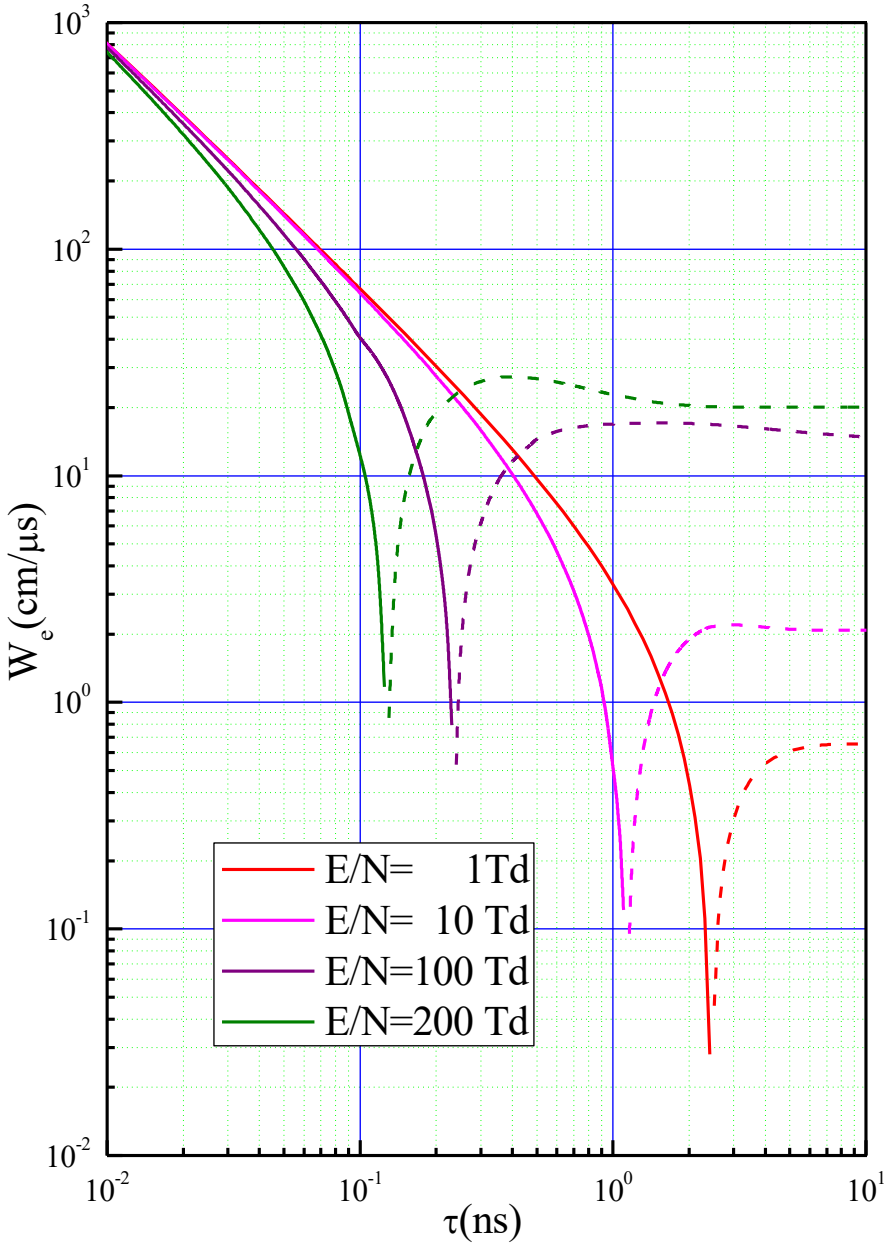

Fig. 2.7. *Electron drift velocity W_e vs time*

Basing on the results obtained we can make the following conclusions:

- The traditional approach to determine HEMP parameters on the base of two goups of electrons generated due to the gamma/X-ray radiation effect on the atmosphere:

  - relativistic electrons (with energies ε ~ 10^6 eV) resulting from Compton scattering of gamma quanta, and

  - low-energy conductivity electrons (with energies ε~1-10 eV),

may be used, if the characteristic time of variations in the gamma flow is $\tau_\gamma \geq 10/\delta$ ns; HEMP parameter calculations for a prompt gamma quanta output require the kinetic approach.

- In case of pre-breakdown intensities of the electric field, it is necessary to use the kinetic approach, because it is the only way to describe the escape of relativistic electrons affecting the radiation-induced conductivity characteristics.

3. HEMP WAVEFORMS CALCULATIONS

To exemplify the developed model application, we give results of parameter calculations for HEMP induced by a model point gamma source. The rate of the quanta yield from the source varies with time in accordance with the law:

$$\Gamma(\tau) = \Gamma_m \frac{(\alpha+\beta)\cdot\exp(\alpha\tau)}{\beta+\alpha\exp[(\alpha+\beta)\cdot\tau]}. \qquad (3.1)$$

The energy spectrum of gamma rays is assumed to be time independent and is described by formula (2.2), which approximates the U^{235} fission spectrum.

The source is located at an altitude H_B above Earth's surface in exponential atmosphere with inhomogeneity scale $H_0 = 7$ km. The geomagnetic field, B_0 is directed at angle θ_B to the vertical. This is a representative problem for studying physical processes associated with the HEMP generation at early times.

3.1. Influence of Multiple Scattering and Self-Consistency on HEMP Characteristics

To illustrate the discrepancy of results obtained with the use of HEMP models accounting for various effects, a number of calculations were performed for the problem below. A point source of gamma rays is located at an altitude of $H_B = 75$ km above the Earth surface. The geomagnetic field B_0=0,5 Gs is parallel to the Earth surface, $\theta_B = 90^\circ$. The observation point is on the Earth surface at a right angle to the geomagnetic field.

Three different models were used in our calculations. The first one was a fully self-consistent model used to solve the Boltzmann equation with consideration of multiple scattering of fast electrons and the generated electromagnetic field effect on the motion of fast electrons. The second model neglects the generated fields in the motion equation for fast electons (no self-consistency). The third model additionally neglects the effect of multiple scattering. Time dependencies of the radiated electric field at the observation point obtained with each of the models above are shown in Fig.4.1. It is clear seen that, if multiple scattering and self-consistency effects are ignored (either separately, or simultaneously), the EMP amplitude and the rate of field rise are overestimated.

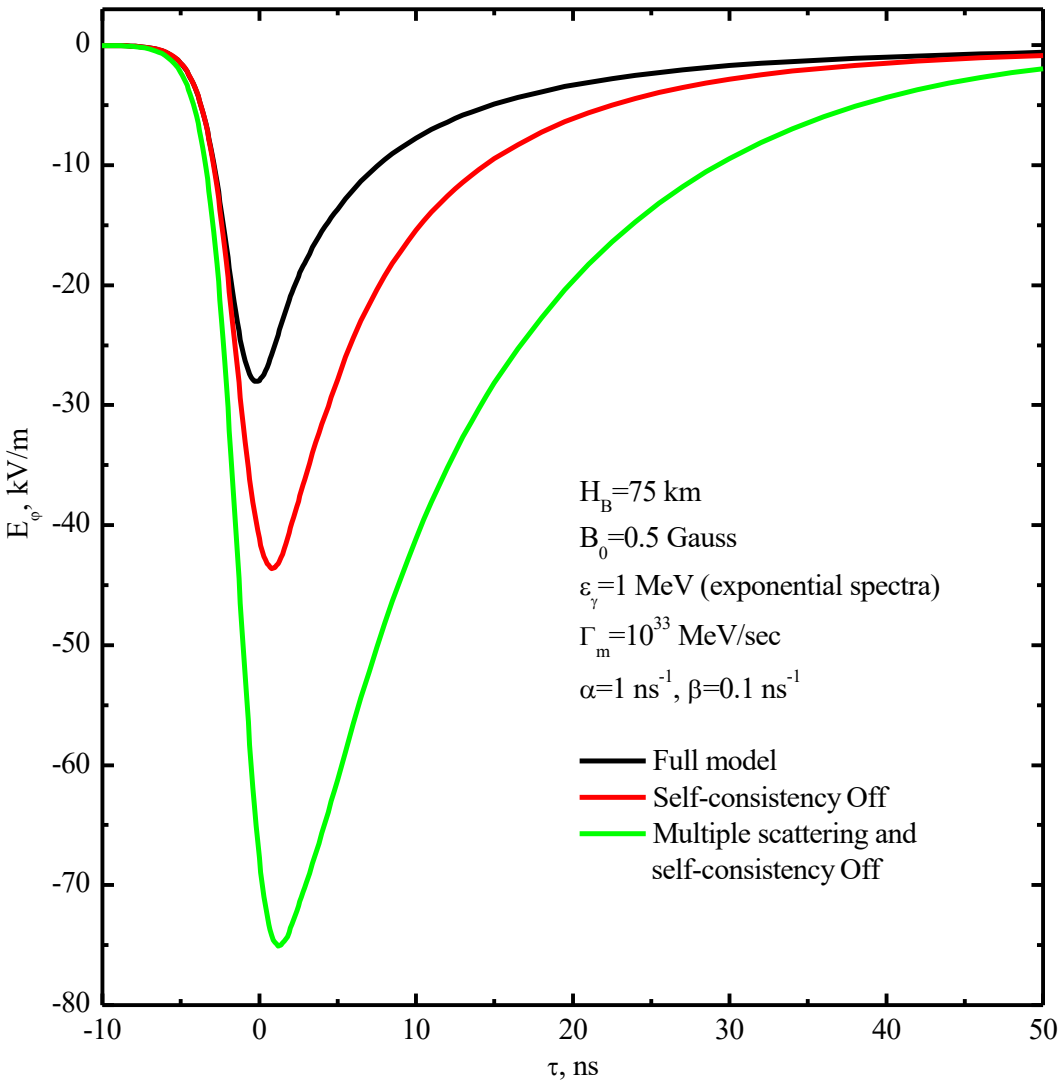

Fig. 3.1 *Time dependencies of radiated electric field obtained using different models*

The common approach to the treatment of the Compton electron currents and air conductivity in the HEMP problem implies that there are two groups of electrons. One group includes primary electrons generated due to the Compton effect, or the photoeffect. Another group includes secondary electrons generated due to the air ionization by primary electrons. Though such division has a clear physical sense, we face difficulties in describing these groups separately. Some of the secondary electrons generated by fast primary electrons have enough energy to produce further ionization. The completion of the residual ionization and thermalization of the distribution of secondaries takes some time (so-called "formative time lag"). This effect may be most important for fast rising pulses because of a lower density of secondary electrons and, therefore, a lower air conductivity for some time. If secondary electrons are described by some preset distribution, there arises the problem of how we can properly select the form of this distribution and its parameters.

The principle of our method is that we do not divide electrons into primary and secondary ones. Our division into fast and slow electrons is associated with the self-consistent solution of Maxwell's equations in combination with the Boltzmann equation for electrons. The conductivity is not considered a separate physical factor influencing the HEMP waveform. The time lag effect is automatically taken into consideration in calculating HEMP parameters using the kinetic approach.

3.2. HEMP Dependence on the Burst Altitude and Gamma Source Intensity

The first series of computations was performed to study the dependence of HEMP parameters on the burst altitude. For a constant peak gamma yield rate, $\Gamma_m = 10^{33}$ MeV/sec, the burst altitude varied within the range of values $H_B = 50-300$ km. The corresponding time dependences of φ-components of the electric field at the ground level are shown in Fig. 3.2. Note that the HEMP amplitude dependence on the source altitude has its maximum $E_{\varphi max} \approx 28$ kV/m at $H_B \approx 75$ km.

In the second series of computations performed at a fixed burst altitude, $H_B = 50$ km, the gamma yield rate varied within the range of values $\Gamma_m = 10^{31}-10^{33}$ MeV/sec. The corresponding dependences of the electric field φ-components on time at the ground level are shown in Fig. 3.3. The HEMP amplitude and rise time increase monotonically with the growth of Γ_m. In particular, for the peak value $\Gamma_m = 10^{33}$ MeV/sec the amplitude is $E_{\varphi max} \approx 23$ kV/m.

Finally, a series of computations was performed to examine the spatial distribution of the HEMP amplitude at a fixed burst altitude $H_B = 75$ km and for a peak intensity $\Gamma_m = 10^{33}$ MeV/sec. In these calculations we assumed $\theta_B = 45^\circ$ - the angle between the geomagnetic field vector and the vertical. Observed points ranged within heights $H = 0-100$ km and ground distances $R = 0-150$ km. The calculated distribution of the HEMP amplitude is shown in Fig. 3.4. Note the two regions of high electric field, which correspond to the source region in the vicinity of the burst point and the deposition region in the altitude range from 20 to 40 km.

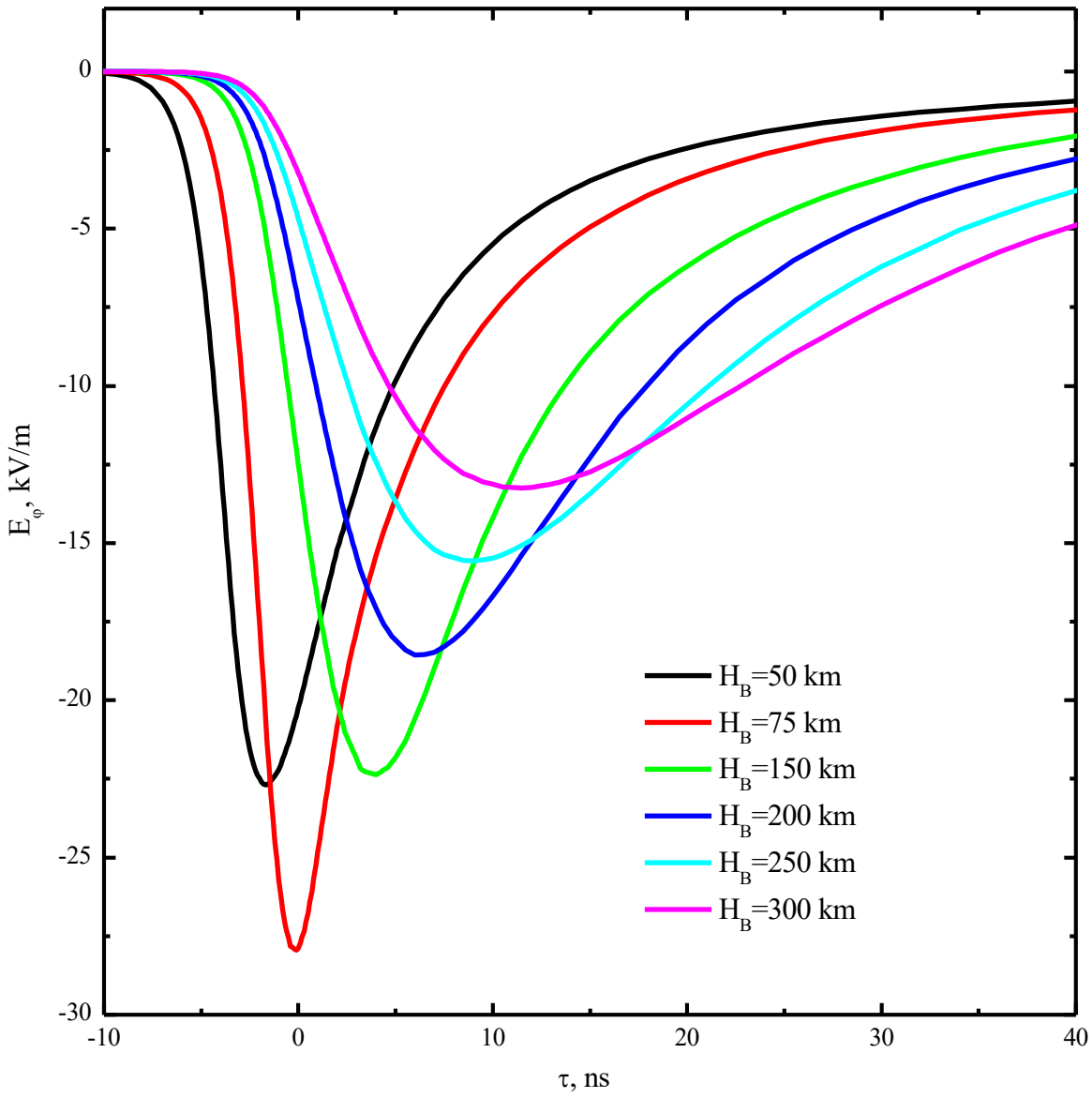

Fig. 3.2. *Time dependencies of radiated electric field for various burst altitudes*.

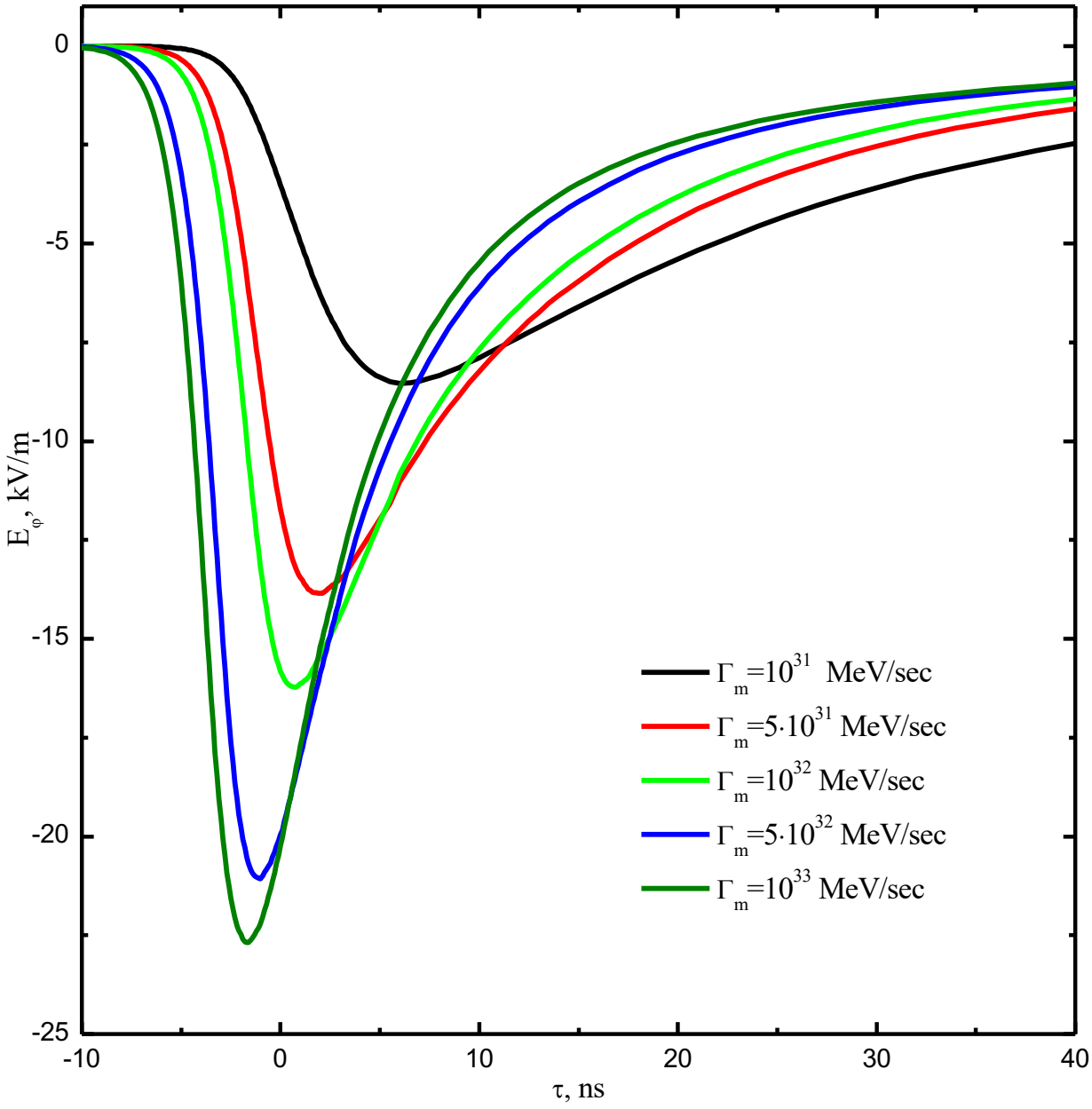

Fig. 3.3. *Time dependencies of radiated electric field for various source intensities*

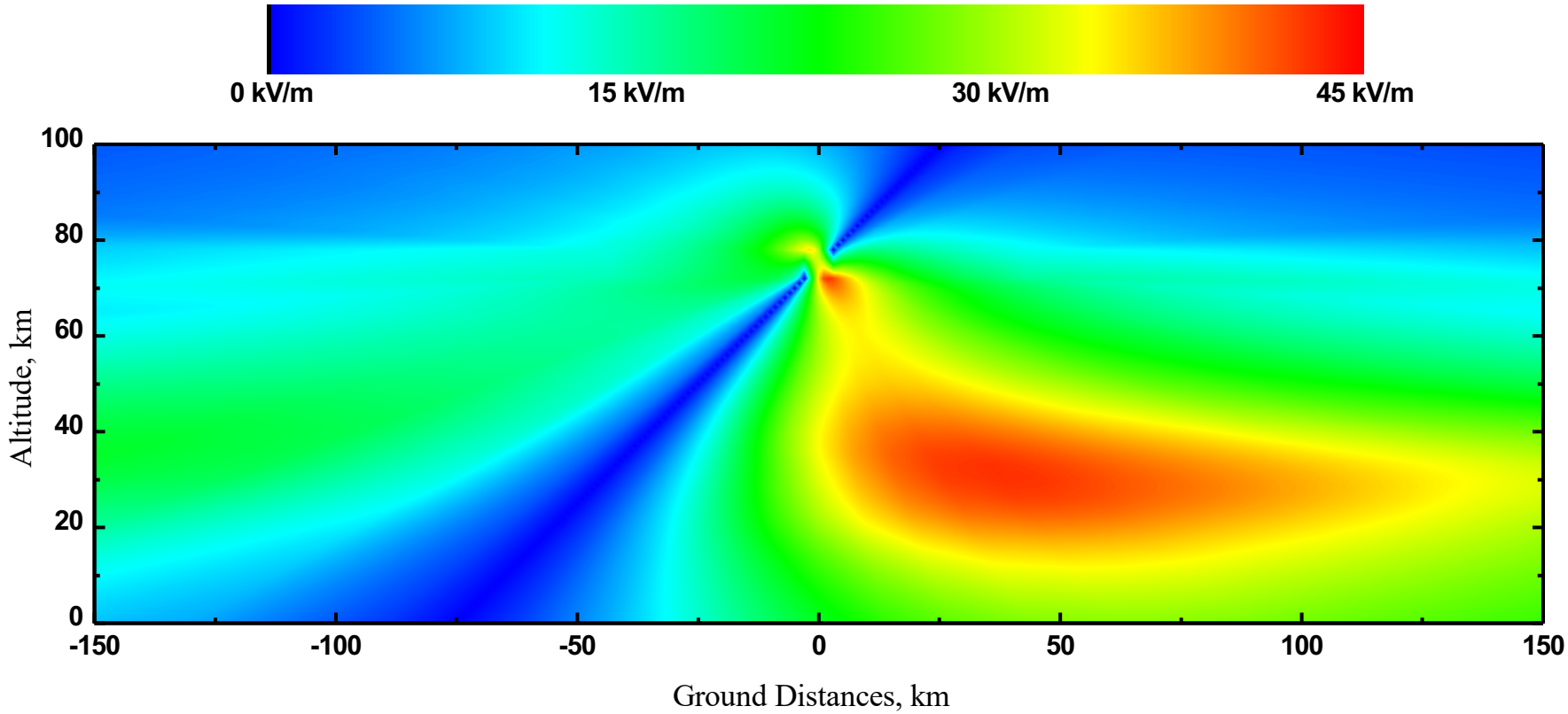

Fig.3.4. Spatial distribution of the radiated electric field amplitude

CONCLUSION

We have developed a model to determine parameters of an electro-magnetic pulse (EMP), generated in air by gamma rays from a high-altitude nuclear explosion. The model is based on a self-consistent solution of the Boltzmann kinetic equation for electrons together with Maxwell's equations. Slow electrons (below several keVs) are described using the elliptic representation of the Boltzmann equation taking into account the process of both elastic and inelastic scattering. Fast electrons (above several keVs) are simulated with the particle method using the relativistic Fokker-Planck approximation. The electron model allows considering the exchange between ensembles of slow and fast electrons. The effect of formative time lag is automatically taken into consideration within the framework of our model. HEMP fields are determined using Maxwell's equations in the high-frequency approximation.

The developed model was applied to examine the role of non-linear, non-steady-state and kinetic effects on the HEMP waveform. In particular, comparative calculations were performed to study the influence of multiple scattering and self-consistent electromagnetic fields on HEMP characteristics. It was found that multiple scattering plays a significant role for all considered parameters of the gamma ray source. Parametric calculations of HEMP induced by a point gamma source at altitudes from 50 to 300 km were presented as an example of the developed model application.

REFERENCES

1. W.J. Karzas and R. Latter, Detection of the Electromagnetic Radiation from Nuclear Explosion in Space, Phys. Rev., Vol. 137, No. 5B, 1965, pp. 1369-1378.
2. R.I. Ilkaev, A.I. Golubev, L.M. Gorshunov, S.S. Zasimov, V.E. Moskalenko, V.N. Pristavko, V.A. Terekhin, Proposals for Collaboration in the Area of Electromagnetic Methods for Verification of Compliance with the Nuclear Weapons Non-Proliferation Treaty, in *Non - proliferation and arms Control Technologies workshop*, Lawrence Livermore National Laboratory, September 16-20, 1996.
3. A.I. Golubev, M.D. Kamchibekov, A.V. Soldatov, T.G. Sysoeva, V.A. Terekhin, V.T. Tikhonchuk, Nonlinear and Kinetic Effects in Propagation of Intense Electromagnetic Pulse through the Atmosphere, Electromagnetic waves and electronic systems, Vol. 3, No. 2-3, 1998, pp. 93-99.
4. A.A. Solovyev, V.A. Terekhin, V.T. Tikhonchuk, L.L. Altgilbers, Electron Kinetic Effects in the Atmosphere Breakdown by an Intense Electromagnetic Pulse, Phys Rev. E, Vol. 60, No. 6, 1999, pp.7360 – 7368.
5. A.I. Golubev, T. G. Sysoeva, V.A. Terekhin, V.T. Tikhonchuk, L.L. Altgilbers, Kinetic Model the Propagation of Intense Subnanosecond Electromagnetic Pulse through the Lower Atmosphere, IEEE Plasma Science, Vol. 28, No. 1, 2000, pp. 303 – 311.

6. A.I. Golubev, M.D. Kamchibekov, A.A. Solovyev, T.G. Sysoeva, A.V. Terekhin, V.A. Terekhin, Nonstationary, Nonlinear and Kinetic Effects Driven by a Powerful EMP in the Earth's Atmosphere, *Proceedings of the Russian Federal Nuclear Center – VNIIEF*. Vol..3, pp. 28-51, 2002.
7. A.V. Gurevich, G.M. Milikh, R.A. Rousel-Dupree, Runaway Electron Mechanism of Air Breakdown and Preconditioning During a Thunderstorm, Phys. Lett., A165, 1992, pp.463-468.
8. D.E. Merewether, W.A. Radasky, Nonlinear Electromagnetic Fields within a Cylindrical Cavity Excited by Ionized Radiation, IEEE Trans. Nucl. Sci., Vol. 21, No. 6, 1974, pp.998–1005.
9. O.V. Osipova, A.A. Solovyev, A.V. Terekhin and V.A. Terekhin, Self-Consistent Problem of Electric Fields Produces in Air by a Gamma Quantums Pulse, in *Youth in a science*, Sarov, 2002, pp.156-167 (in Russian).
10. E. A. Richley, Elliptic Prepresentation of the Boltzmann Equation with Validity for All Degrees of Anisotropy, Phys. Rev. E, 59, 4533 (1999).
11. C.D. Zerby, F.L. Keller, Electron Transport Theory, Calculation and Experiment, Nucl. Sci. Eng., Vol.29, 1967, p.151.
12. C.L. Longmire, H.J. Longley, Improvements in the Treatment of Compton Current and Air – Conductivity in EMP Problems, Defense Nuclear Agency Report DNA 3192T, 1973.
13. C.L. Longmire, State of the Art in IEMP and SGEMP Calculations, IEEE Trans. Nucl. Sci., Vol. 22, No. 6, 1975, pp. 2340–2344.
14. E. Storm, H. Israel, Photon cross sections from 0.001 to 100 MeV for elements 1 through 100, Los Alamos Scientific Laboratory, N.M., 1967.
15. B.R. Suydam, *Early Radio Flash from a Low-Altitude Air Burst*, LA-4245-MS, Los Alamos Scientific Laboratory, 1970.
16. J. Datton, A Survey of Electron Swarm Data, J. Phys. Chem. Ref. Data, Vol.4, No.3, 1975, pp. 577-856.
17. H. Hasegawa, H. Date, Y. Ohmori, P.L.G. Ventzek, M. Shimozuma, H. Tagashira, Measurements of the drift velocity of electrons in mixtures of nitrogen and carbon dioxide from 100 to 1000 Td, J. Phys D: Appl. Phys. Vol.31, No.6, 1998, pp.737-741.
18. A.B. Wedding, H.A. Blevin, J. Fletcher, J. Phys D: Appl. Phys. Vol.18, No.12, 1985, pp.2361-2373.
19. W. Roznerski, K. Leja, Electron drift velocity in hydrogen, nitrogen, oxygen, carbon monoxide, carbon dioxide and air at moderate E/N, J. Phys D: Appl. Phys. Vol.17, No.2, 1984, pp.279-285.

20. S.A.J. Al-Amin, J. Lucas, H.N. Kucukarpaci, The ratio of radial diffusion coefficient to mobility for electrons in hydrogen, nitrogen and carbon monoxide at high E/N, J. Phys D: Appl. Phys. Vol.18, No.10, 1985, pp.2007-2016.
21. A.B. Wedding, H.A. Blevin, J. Fletcher, The Transport of Electrons through Nitrogen Gas, J. Phys D: Appl. Phys. Vol.18, No.12, 1985, pp.2361-2373.
22. S.C. Haydon, O.M. Williams, Combined Spatial and Temporal Studies of Ionization Growth, J. Phys D: Appl. Phys. Vol. 9, № 3, 1976, pp.523-536.
23. S.A.J. Al-Amin, H.N. Kucukaraci and J. Lucas, Electron Swarm Parameters in Oxygen, and Methane, J. Phys. D: Appl. Phys., Vol.18, No. , 1985, pp.1781 – 1794.
24. L.G.H. Huxley, O.M. Crompton, The Diffusion and Drift of Electron in Gases, A Wiley-Interscience Publ., 1977.
25. M.S. Naidu, A.N. Prassad, Mobility Diffusion and Attachment of Electron in Oxygen, J.Phys. D, 3, 957-964, (1977)
26. A.N. Prasad, J.D. Craggs, Measurement of Townsend's Ionization Coefficients and Attachment Coefficients in Oxygen, Proc. Phys. Soc. London, 77, 385-398, (1961)
27. M.A. Harrison, R. Geballe, Simultaneous Measurement of Ionization and Attachment Coefficients, Phys.Rev., 91, 1-7, (1953)